

Models of spatial and orientational self-organization of microtubules under the influence of gravitational fields

S. Portet* and J. A. Tuszyński

Department of Physics, University of Alberta, Edmonton, Alberta, Canada T6G 2J1

J. M. Dixon

Department of Physics, University of Warwick, Coventry CV4 7AL, United Kingdom

M. V. Sataric

Faculty of Technical Sciences, University of Novi Sad, 21000 Novi Sad, Serbia, Federal Republic of Yugoslavia

(Received 15 January 2003; published 11 August 2003)

Tabony and co-workers [C. Papaseit, N. Pochon, and J. Tabony, Proc. Natl. Acad. Sci. U.S.A. **97**, 8364 (2000)] showed that the self-organization of microtubules from purified tubulin solutions is sensitive to gravitational conditions. In this paper, we propose two models of spatial and orientational self-organization of microtubules in a gravitational field. First, the spatial model is based on the dominant chemical kinetics. The pattern formation of microtubule concentration is obtained (1) in terms of a moving kink in the limit when the disassembly rate is negligible, and (2) for the case of no free tubulin and only assembled microtubules present. Second, the orientational pattern of striped microtubule domains is consistent with predictions from a phenomenological Landau-Ginzburg free energy expansion in terms of an orientational order parameter.

DOI: 10.1103/PhysRevE.68.021903

PACS number(s): 82.20.-w, 82.70.-y, 82.39.-k, 89.75.Kd

I. INTRODUCTION

Microtubules (MT's) are major cytoskeletal proteins and are present in virtually all eukariotic cells. They are involved in many essential cell functions such as mitosis, maintenance of cell shape, cell motility, signal transduction, and intracellular transport. MT's exhibit a highly dynamical behavior and specific spatial reorganizations which allow them to perform their cellular roles. MT's are long cylindrical polymers that exhibit aggregation through the addition at their ends of α , β -tubulin heterodimers [1].

Tabony and co-workers have conducted a series of experiments on the effects of the gravitational conditions on the *in vitro* self-organization of MT's under conditions of high tubulin concentration [2,3]. Preparations containing purified tubulin and GTP (guanosine triphosphate) were heated from $\approx 7^\circ\text{C}$ to 37°C and MT's were assembled in rectangular samples of particular size ($40 \times 10 \times 1 \text{ mm}^3$). An enzymatic system was also present to regenerate the GDP (guanosine diphosphate) and to provide a continuous source of GTP. The different samples were subjected to specific gravitational conditions. Thus, progressive self-organization of MT's was observed depending on the gravitation field strength and the orientation of samples with respect to the gravity axis. These authors [2,3] observed that after about 5 h, the preparations had stabilized and the following types of pattern of MT assembly had been identified: (1) under gravity (on Earth and in flight under 1g centrifugation) with the major axis of the

sample parallel to the gravity axis, striped patterns of MT's appeared, with two adjacent stripes made up of highly oriented MT bundles at an angle of 45° and 135° , respectively, to the horizontal (Fig. 1); (2) under gravity and with the major axis of samples perpendicular to the gravity axis, circular patterns were observed; (3) in weightlessness ($10^{-4}g$), an isotropic pattern appeared, and no preferential orientation was adopted by the MT's.

The effect of the gravitational field on the MT self-organization has been observed both for *in vitro* and *in vivo* experiments with mammalian and vegetal specimens. For example, in two different space flight experiments led by Lewis [4] and Vassy [5], the structural organization of *in vivo* MT's showed dramatic differences between the gravity and microgravity conditions. Instead of well-formed MT's radiating from organizing centers in the gravitational environment, cells in microgravity uniformly diffuse and exhibit shortened MT's without normal organization.

In the present paper, we construct models in accordance with the experimental conditions outlined in Ref. [6], to describe quantitatively the effects of the gravitational field on the self-organization of MT's. Two distinct approaches will be presented dealing separately with the spatial distribution of the MT concentration and with orientational order within the MT assembly. The reason for this distinction is the presence of the vastly different time scales of these two different dynamical processes, the former being much faster than the latter due to the significant differences between the diffusion constants for tubulin and MT's, respectively.

II. THE MODEL OF SPATIAL ORGANIZATION

To model the spatial self-organization of *in vitro* MT's, we consider the competition between different processes. These include nonlinear chemical kinetics of MT assembly

*Author to whom correspondence should be addressed. Present address: Samuel Lunenfeld Research Institute, Mount Sinai Hospital, 600 University Ave., Toronto, Canada M5G 1X5. Email address: sportet@mshri.on.ca sportet@phys.ualberta.ca

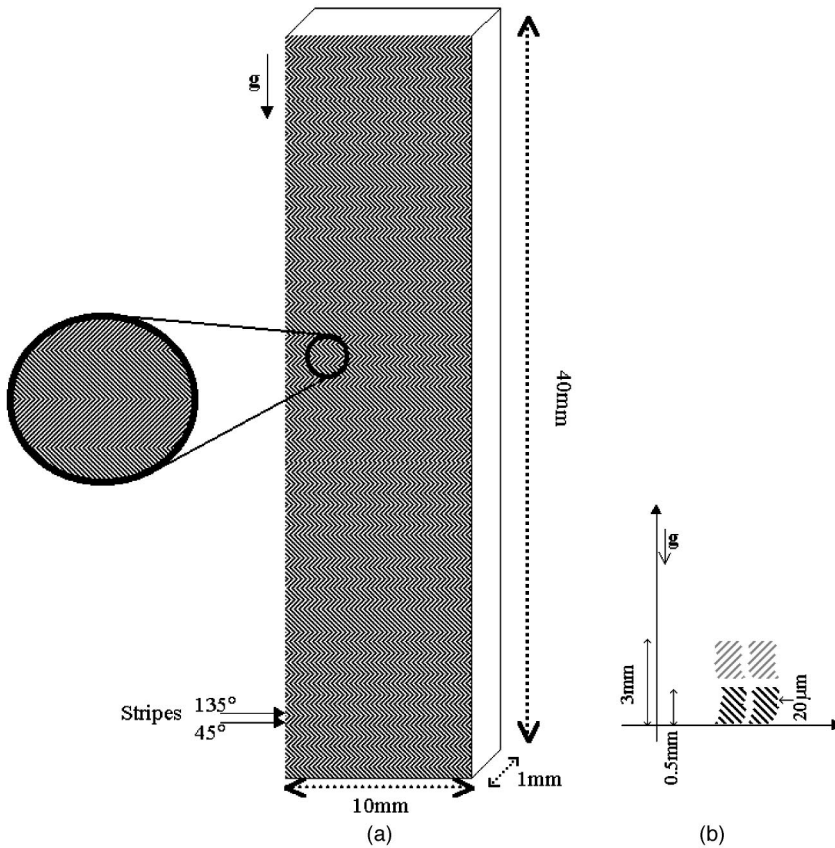


FIG. 1. (a) After about 5 h in the experiments reported in Ref. [2], striped patterns of MT's appeared, with two adjacent stripes made up of highly oriented MT bundles at an angle of 45° and 135°, respectively, to the horizontal. (b) The characteristic spatial periodicities developed within stripes for the samples exposed to gravity during the first 6 min, with the major axis of the sample parallel to the gravity axis.

[7,8], diffusion processes of tubulin and MT's accounting for significant differences in the diffusion coefficient as a result of size and geometrical characteristics, and a hydrodynamic drift process of tubulin dimers and MT's resulting from the action of the gravitational field with the buoyancy correction [9]. To develop a physical model, we use a reaction-diffusion approach that accounts for the gravitational environment. The model equation is generally expressed by

$$\frac{\partial S}{\partial t} = \underbrace{D\nabla^2 S}_{\text{Diffusion}} - \underbrace{u \cdot \nabla S}_{\text{Drift induced by gravity}} + \underbrace{R(S)}_{\text{Chemical reactions}}, \quad (1)$$

where S is the two-vector of the concentrations C and M , C is the number concentration of tubulin dimers, and M is the number concentration of MT's. D is the diagonal matrix of positive diffusion constants. u is the diagonal matrix of drift velocities of proteins induced by gravitational conditions. R is the two-vector of the reaction terms $f(C, M)$ and $h(C, M)$ that are described below in detail. The present model is considered with the initial conditions $\forall x \in \Omega$, where Ω is the spatial domain, $C(x, 0) = c_0$, $M(x, 0) = 0$, and zero-flux boundary conditions are used.

In the development of the reaction term, we are guided by the tools of chemical kinetics as applied to protein polymerization. The reader is referred to the seminal works of Hill [7] and Oosawa and Asakura [8]. Furthermore, in the present study we wish to strongly emphasize the emergence of spatial patterns that were observed by Tabony and Job [3].

Hence, our focus is on the observed dynamics of MT aggregation. With the inclusion of free tubulin dynamics that drives MT aggregation, we therefore need to distinguish two principal state variables: the assembled tubulin and the free tubulin. In our model, chemical kinetics equations are proposed in terms of number concentration for the free dimer tubulin, $C(\cdot)$, and for MT's, $M(\cdot)$.

MT's switch between assembly and disassembly phases. This behavior is called dynamic instability [1], the transition from disassembly to assembly phases is known as *rescue* and the reverse process, i.e., the transition from assembly to disassembly, as *catastrophe*. Moreover, we assume the presence of spontaneous *nucleation* from nuclei (can also be called seeds) which initiate MT's. The kinetics of MT nucleation was studied in detail by Flyvbjerg *et al.* [10]. We also include the possibility of a nucleus elimination reaction, i.e., the reverse chemical reaction that removes MT's from the solution because the nuclei may become structurally unstable. Thus the dynamics of the number of MT's will only depend on this reversible reaction. On the other hand, the dynamics of free tubulin will also be determined by the alternation of catastrophes and rescues, while the gradual shortening and elongation processes will be ignored due to their shorter time scale and limited effect on the process of MT aggregation. While individual MT's exhibit catastrophes and rescues, this polymerization behavior becomes smoothed out and is not so dramatic for ensembles at high concentrations. Nonetheless, there exist collective phases of assembly and disassembly for MT aggregates and our objective in this

paper is a coarse-grained approach that focuses on these collective phenomena. Somewhat similarly but in the study of a different effect, Jobs *et al.* [11] developed an accurate model for MT oscillation dynamics. During disassembly events, MT's release GDP-tubulin which must be recycled as GTP-tubulin to be used again to form a MT. Thus the inclusion of GTP and GDP concentrations as well as GDP-tubulin and GTP-tubulin species is necessary in the complete theoretical description of MT dynamics. However, the experimental conditions considered here, i.e., the presence of a GTP-regenerating system that provides a continuous source of GTP [3], results in a constant GTP concentration in the sample. This leads us to consider, for the purpose of the present model, a simplification of the recycling of GDP-tubulin as an instantaneous process as well as to ignore the difference between the GTP-tubulin and GDP-tubulin pools. Thus, we have opted to account for the recycling process, which also includes the effect of turnover, by introducing an effective term that is proportional to the tubulin concentration. As motivated above by the underlying chemical kinetics, we postulate the following reaction terms in Eq. (1):

$$f(C, M) = - \underbrace{nk_n C^n}_{\text{nucleation}} - \underbrace{k_+ CM}_{\text{assembly}} + \underbrace{nk_{-n} M}_{\text{nucleus elimination}} + \underbrace{k_- M}_{\text{disassembly}} + \underbrace{k_1 C}_{\text{recycling}} \quad (2a)$$

and

$$h(C, M) = \underbrace{k_n C^n}_{\text{nucleation}} - \underbrace{k_{-n} M}_{\text{nucleus elimination}}, \quad (2b)$$

where k_+ is the assembly rate, k_- is the disassembly rate, k_n is the nucleation rate, k_{-n} is the rate of nucleus elimination, and k_1 is the recycling rate for tubulin. Note that k_+ and k_- should not be misconstrued to represent the related kinetics coefficients for a single MT. The present values jointly describe the effective rate of the individual process and the frequency of occurrence. Here, n is the critical number of tubulin dimers necessary for the MT nucleation. The process of MT nucleation is a slower process than assembly. Structurally speaking, it is a more nonlinear process than either assembly or disassembly. While nucleus elimination and disassembly terms in Eq. (2a) can be linked together mathematically, they represent a different effect and are governed by a different dynamics. Nucleation processes, on the other hand, cannot be combined with other effects. It should also be mentioned that the presence of recycling terms is analogous to an additional compartment in the so-called compartmental models resulting in a delay of the assembly process. All the rate constants are positive.

The drift velocity u_i for a particle of type i is calculated according to $u_i = (D_i/k_B T) f_i$, where D_i is the diffusion coefficient of the molecule of type i , k_B is the Boltzmann constant, and T is the temperature (in kelvin). The term f_i represents the net force (force of gravity and force of buoyancy)

that acts on a molecule of type i : $f_i = m_i(1 - \rho_\epsilon/\rho_i)g$, where m_i is the molecular mass, ρ_ϵ is the mean density of the solution, ρ_i is the density of molecules, and g is the strength of the gravitational field.

The competition between hydrodynamic forces due to the sedimentation process and Brownian motion acting on each type of particle is characterized by the Peclet number Pe defined as follows [12]:

$$Pe = \frac{r_i u_i}{D_i} = \frac{r_i f_i}{k_B T}, \quad (3)$$

where r_i is the diameter of the molecule. When $Pe \ll 1$, the diffusion process dominates over the directional transport, and the latter can be considered insignificant within the sample. It is assumed that the solution is an aqueous buffer, and that the α, β -tubulin heterodimer is approximated by a spherical particle of diameter $r_C = 8$ nm with a mass $m_C = 100$ kDa [1]. We estimate the MT mass by assuming that it is a hollow cylinder (the interior diameter of about 14 nm and the exterior diameter of about 25 nm) of $5 \mu\text{m}$ length [2], made up of 1625 dimers per $1 \mu\text{m}$ length of a MT. The Peclet number for tubulin dimers at 37°C is calculated as $Pe = 10^{-10}$, while for MT's we obtain $Pe = 10^{-2}$. Thus, the drift induced by gravitational conditions can be neglected in the case of tubulin dimers, but it is very relevant for the MT's and dominates the diffusion process.

Consequently, the model in Eq. (1) is now expressed in the one-dimensional case (along the gravity axis) by two coupled nonlinear partial differential equations

$$\frac{\partial C}{\partial t} = D_C \frac{\partial^2 C}{\partial x^2} + f(C, M), \quad (4a)$$

$$\frac{\partial M}{\partial t} = -\Gamma \frac{\partial M}{\partial x} + h(C, M), \quad (4b)$$

where D_C is the diffusion coefficient of tubulin dimers. Extrapolating from the tubulin diffusion coefficient measured for *in vivo* sea urchin eggs at 25°C as $5.9 \times 10^{-12} \text{ m}^2 \text{ s}^{-1}$ [13], we estimate $D_C = 70 \times 10^{-12} \text{ m}^2 \text{ s}^{-1}$ under the experimental conditions [2] considered here. In the experiments, the temperature was 37°C rather than 25°C , so to obtain this estimate we have scaled the sea urchin diffusion constant, found in Ref. [13], by the ratio of the two temperatures and the ratio of the corresponding viscosities at these two temperatures.

The drift coefficient $\Gamma = \gamma u_M$, where $u_M = (D_M/k_B T) m_M(1 - \rho_\epsilon/\rho_M)g$ is the positive drift velocity for a MT of $5 \mu\text{m}$ in length. From the well-known Stokes-Einstein formula, using the combination of the parallel and perpendicular components of the drag coefficient, we estimate the MT diffusion coefficient to be $D_M = 1.54 \times 10^{-12} \text{ m}^2 \text{ s}^{-1}$. Thus u_M is found to be equal to $5 \times 10^{-10} \text{ m s}^{-1}$ or 30 nm/min .

The scaling parameter γ models the coupling between MT's and the so-called avalanche correlated clusters [14]. Tubulin dimers are negatively charged globular proteins that

are highly screened by positive counterions of the solvent. The thermal fluctuations of the countercharges on tubulins cause a van der Waals attractive force that acts at short distances and induces the aggregation of tubulin dimers. These forces correlate to initiate catastrophic events enabling tubulin dimers to form avalanche correlated clusters.

We are interested in finding the propagation of a pattern of MT assembly through the sample which is subjected to the field of gravity. Hence, we look for constant traveling wave front solutions of Eq. (4b) by defining $M(x,t) = M(x-vt) = M(\xi)$, where v is the wave speed. Substituting this form in Eq. (4b), we obtain the ordinary differential equation

$$(\Gamma - v)M' = k_n C^n - k_{-n} M, \quad (5)$$

where the prime represents differentiation with respect to the moving coordinate ξ . Setting $v = \Gamma$ (note that based on the above, Γ is proportional to the gravitation constant g), we obtain

$$M = \frac{k_n}{k_{-n}} C^n, \quad (6)$$

which allows us to decouple the two equations of the system, Eq. (4). Hence substituting Eq. (6) in Eq. (4a), we obtain

$$\frac{\partial C}{\partial t} - D_C \frac{\partial^2 C}{\partial x^2} = -\frac{k_+ k_n}{k_{-n}} C^{n+1} + \frac{k_- k_n}{k_{-n}} C^n + k_1 C, \quad (7)$$

which is a diffusion equation, with a nonlinear source term, considered with the initial condition $\forall x \in \Omega = \{x: 0 \leq x \leq L_\Omega\}, C(x,0) = c_0$, i.e., starting with a constant tubulin concentration in the sample, and with zero-flux boundary conditions.

Below, we first find special analytical solutions to Eq. (7) under the so-called *domino effect* and second we study the dissipative instability of a homogeneous steady state of Eq. (7), $C^* = 0$, which represents the absence of free tubulin and only assembled MT's in the sample.

A. The domino effect

By considering C as a traveling wave, i.e., as a function of $x - vt = \xi$, and neglecting the term proportional to k_- (since $45 \approx k_- \ll k_+ C \approx 3200$), Eq. (7) may now be expressed by the ordinary differential equation

$$D_C C'' + v C' = \frac{k_+ k_n}{k_{-n}} C^{n+1} - k_1 C. \quad (8)$$

Rescaling by $\tilde{\xi} = \sqrt{D_C/k_1} \xi$ and $\tilde{C} = (k_+ k_n / k_{-n} k_1)^{1/n} C$, Eq. (8) becomes

$$C'' + \frac{v}{\sqrt{D_C k_1}} C' = C^{n+1} - C = C(C^n - 1). \quad (9)$$

The ordinary differential equation (9) has the form of an anharmonic dissipative oscillator equation as follows:

$$C'' + \alpha C' = C(C^n - 1) \quad (10)$$

and, remarkably, its analytical solution is, according to Ref. [15],

$$C = 2^{-2/n} \left[1 - \tanh \left(\frac{n}{2\sqrt{2n+4}} (\xi - \xi_0) \right) \right]^{2/n}, \quad (11)$$

where ξ_0 is an arbitrary constant and $\alpha = -(n+4)/\sqrt{2n+4}$. The wave velocity is dependent on the critical number n of dimers constituting a nucleus according to $v = \alpha \sqrt{D_C k_1}$, where $k_1 = 2 \text{ s}^{-1}$ [16]. This dependence corroborates the well-known insight that the MT nucleation is a major mechanism for determining the spatial organization of MT's. For a given n , we can calculate the wave velocity v . For example, for a critical number $n=6$ (n is considered to lie between 3 and 13, see, e.g., Ref. [10]), the wave velocity is found to be $|v| = 2.96 \times 10^{-5} \text{ m/s}$ (Fig. 2). Thus, in 6 min, the critical time observed in the Tabony experiment, the assembly wave of MT's travels through $10.6 \times 10^{-3} \text{ m}$ and completely crosses the sample [whose width is 10^{-2} m , see Fig. 1(a)]. Therefore, we propose to refer to this phenomenon as the domino effect.

The above solution is admittedly a special solution but to the best of our knowledge it is the only solitary wave that can be found for this type of differential equation. It is interesting to explore the issue of physical stability of Eq. (9) through a phase space analysis. To this end, a phase plane analysis of Eq. (9) may be undertaken by putting

$$C' = Y \quad (12a)$$

and

$$Y' = -\frac{v}{\sqrt{D_C k_1}} Y + C(C^n - 1). \quad (12b)$$

The critical points in the (C, Y) phase plane are the following: a stable point $(0,0)$ and a saddle point $(1,0)$. Figure 3 illustrates the phase plane trajectories and represents both the stable and saddle points. Consequently in mathematical terms, we see that the propagating kink represents a transition from a saddle point to a stable focus point. Physically, we interpret this domino effect solution as a propagating front separating the region with free tubulin and no MT's on the one hand and no free tubulin and only assembled MT's on the other.

Subsequently, the question arises whether in the region of assembled MT's spatially ordered patterns may develop as a result of slow translational but also rotational diffusion processes. This issue will be addressed in Sec. III.

B. Nonhomogeneous perturbation near $C^* = 0$

We are interested in finding the MT pattern formation in Eq. (7). In other words, we wish to focus on the system in the vicinity of the steady state $C^* = 0$ (no free tubulin and only assembled MT's). To examine the effect of small nonhomogeneous perturbations of this steady state, which could be due to thermal agitation or sample imperfections, we consider $\tilde{C}(x,t)$ to be a small perturbation of C^* such that

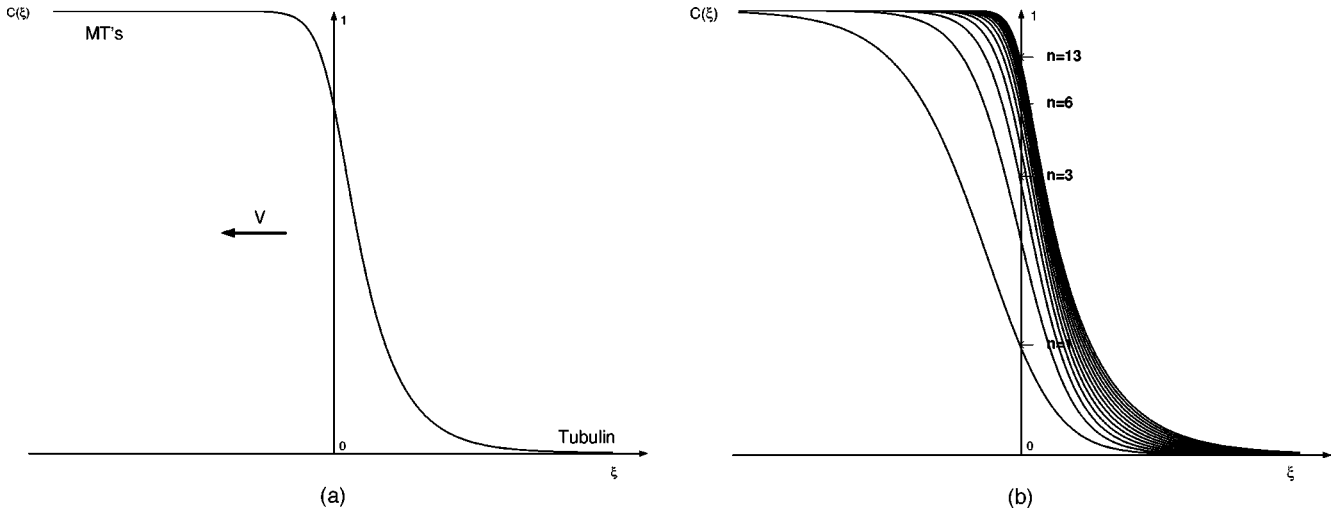


FIG. 2. (a) Plot of Eq. (11) for $n=6$: the wave velocity $|v|=2.96 \times 10^{-5}$ m/s. Thus in 6 min, the wave front travels 10.6×10^{-3} m which is approximately the width of the sample in Tabony experiments. (b) Traveling wave front solutions for Eq. (7) for different wave velocities according to the critical number of dimers required for nucleation. The smaller the critical number, the faster the wave moves.

$$C(x,t) = C^* + \tilde{C}(x,t). \quad (13)$$

For $\tilde{C}(x,t)$ sufficiently small, Eq. (7) can be linearized about the homogeneous steady state C^* by substituting Eq. (13) in Eq. (7) to obtain

$$\frac{\partial \tilde{C}}{\partial t} - D_C \frac{\partial^2 \tilde{C}}{\partial x^2} = k_1 \tilde{C}, \quad (14)$$

where the tilde is omitted for simplicity. The result of linearization in Eq. (14) is to be considered with the same initial conditions and the same zero-flux boundary conditions as before.

By satisfying boundary conditions, we look for solutions of Eq. (14) having the form

$$C(x,t) = \sum_n \tilde{c}_n e^{\omega t} \cos\left(\frac{n\pi}{L}x\right). \quad (15)$$

Here ω determines the temporal growth. By substituting Eq. (15) into Eq. (14) and by canceling $e^{\omega t} \cos[(n\pi/L)x]$, we obtain $\omega = k_1 - D_C(n\pi/L)^2$, so the solution of Eq. (14) is given by

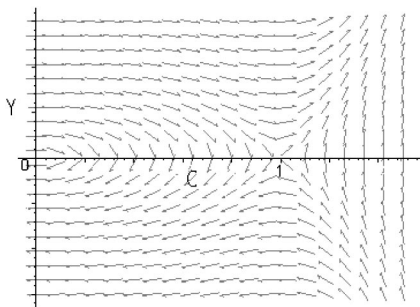


FIG. 3. Phase plane trajectories for Eq. (9) for the traveling wave front solutions, where $v=5 \times 10^{-10}$ m/s= u_M . Traveling wave solutions from $C=1$ (no MT's) to $C=0$ (no tubulin) appear.

$$C(x,t) = \sum_n \tilde{c}_n e^{[k_1 - D_C(n\pi/L)^2]t} \cos\left(\frac{n\pi}{L}x\right), \quad (16)$$

where \tilde{c}_n are proportional to the Fourier series expansion coefficients.

For the steady state $C^*=0$ (no tubulin and only assembled MT's) to be unstable to spatial disturbances, we require the condition $\text{Re}(\omega) > 0$, for some modes $n \neq 0$ (when $n=0$, there will be no spatial effects). Note that the latter also is dependent on the domain size L . Thus we can calculate the critical size L_c of the spatial domain, for which the system becomes unstable. We require the largest ω for which the system is unstable [$\text{Re}(\omega)=0$]. This means $n=1$, the smallest mode. Thus the critical size L_c is expressed as

$$L_c = \pi \sqrt{\frac{D_C}{k_1}}. \quad (17)$$

Therefore, when $L > L_c$, there exist ranges of unstable modes n , where spatial structure appears (Fig. 4). In our case, as $L_c = 1.9 \times 10^{-5}$ m and the domain size is at least $L = 10^{-3}$ m, pattern formation is expected to arise as described above. Note that this length scale corresponds to an observed spatial periodicity in MT bundles measured by Tabony as $20 \mu\text{m}$ [Fig. 1(b)] [2].

Once MT's have been formed and have achieved their full length at saturation, they are likely to interact with other MT's in solution via several physical forces. First of all, there are excluded volume effects due to the significant size of MT's reaching a length of $5 \mu\text{m}$ or more. While their average center-to-center distance for the experimental conditions considered here is of the order of 100 nm , the preferred orientation for MT assemblies is parallel [2]. This will be enforced by the electrostatic effects due to the net charge on the surface of each MT. When the surface charge density is of the order of $\sigma \approx 0.5 \text{ e/nm}^2$, it yields electrostatic repulsion

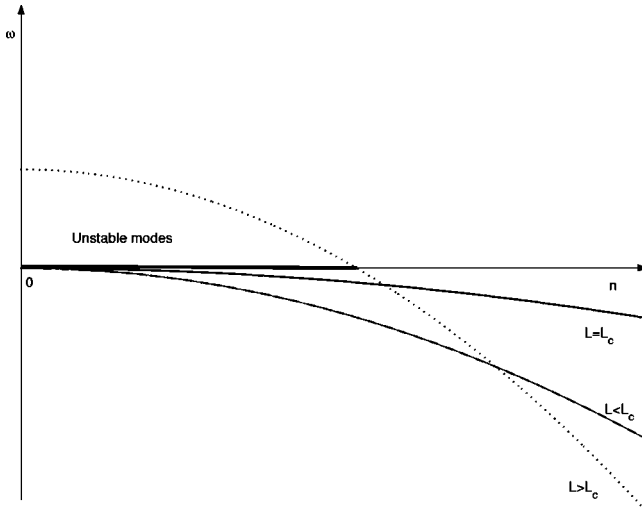


FIG. 4. Representation of the eigenvalues ω as a function of n . When $L > L_c$, there is a range of modes which are unstable.

forces that are significant (of the order of 10 pN) even when Debye screening due to the ions in solution is accounted for. All of these factors will introduce orientational ordering which we discuss in the following section.

III. ORIENTATIONAL ORDERING

In the previous sections of the paper, we introduced two dependent variables characterizing the assembly processes taking place in the sample. These variables C and M referred to the concentrations of tubulin and MT's, respectively, and are taken to be non-negative scalar variables. However, once MT-MT interactions are included in the ordered state of the MT assembly, it is more appropriate to characterize the local concentration of MT's as a complex order parameter, to use the language of the theory of phase transitions [17]. This is very similar to the case of nematic liquid crystals which are composed of long rodlike molecules forming an anisotropic fluid. For liquid crystals, the order parameter for the formation of parallel rolls is the so-called director field. However, various defect structures commonly emerge in anisotropic fluids under the influence of external fields and their ordering can be characterized by an angle θ that measures orientational deviation from the director axis. Hence, we introduce a complex order parameter for the orientational ordering of the MT assembly as

$$\Psi(x,t) = M(x,t)e^{i\theta(x,t)},$$

where $M(x,t)$ is the MT concentration and $\theta(x,t)$ shows a spatiotemporal deviation from a preferred ordering direction for an MT assembly.

Similarly to nematic liquid crystals, we postulate the existence of a free energy functional in terms of θ that captures the essential features of the MT-MT interactions in the system. The functional takes the well-known Landau-Ginzburg form:

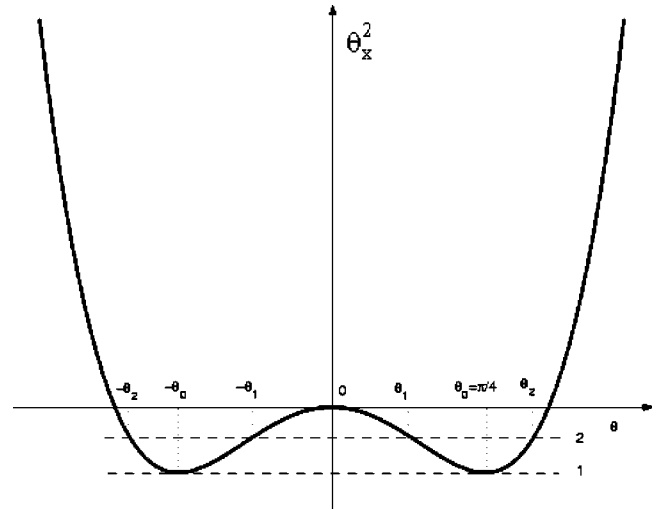


FIG. 5. A plot of θ_x^2 versus θ with the two types of solution indicated and labeled 1 and 2 where 1 is $\theta(x) = \theta_0 \tanh(\alpha x)$ and 2 is $\theta(x) = \theta_1 \text{sn}(\beta x, k)$.

$$F(\theta, \theta_x) = \int \left[-\frac{A}{2} \theta^2 + \frac{B}{4} \theta^4 + \frac{D}{2} \theta_x^2 \right] dx, \quad (18)$$

where $\theta_x = \partial\theta/\partial x$ and A , B , and D are phenomenological expansion parameters to be fitted to experimental data. In our case, the x axis is along the field of gravity. We assume here that the amplitude of the order parameter, $M(x,t)$, is approximately constant and only its phase θ varies once the initial process of MT spatial assembly has been completed.

Minimizing the free energy F with respect to θ leads to the Euler-Lagrange equation of the form

$$D\theta_{xx} = -A\theta + B\theta^3. \quad (19)$$

This equation can be integrated once to give

$$\frac{D}{2} \theta_x^2 = -\frac{A}{2} \theta^2 + \frac{B}{4} \theta^4 + C_0, \quad (20)$$

where C_0 is an integration constant setting the energy scale for a given solution $\theta(x)$. In Fig. 5, we plot the variable θ_x^2 on the left hand side of this equation as a function of the variable θ . In general, this equation can be mapped onto a standard elliptic form.

Importantly from the physical point of view, there exist two nonsingular real types of solution $\theta(x)$ of Eq. (20) [18]:

(a) First type: kink-type domain walls given by

$$\theta(x) = \pm \theta_0 \tanh(\alpha x), \quad (21)$$

where $\theta_0 = \sqrt{A/B}$ and $\alpha = \sqrt{A/2D}$. This solution is shown in Fig. 6.

(b) Second type: periodic solutions expressed via the Jacobi elliptic function $\text{sn}(x,k)$ [see as an example, Fig. 7(a)]:

$$\theta(x) = \theta_1 \text{sn}(\beta x, k), \quad (22)$$

where θ_1 is the smaller of the two positive real roots of the equation $-(A/2)\theta^2 + (B/4)\theta^4 + C_0 = 0$, and $\beta = \theta_2 \sqrt{B/2D}$

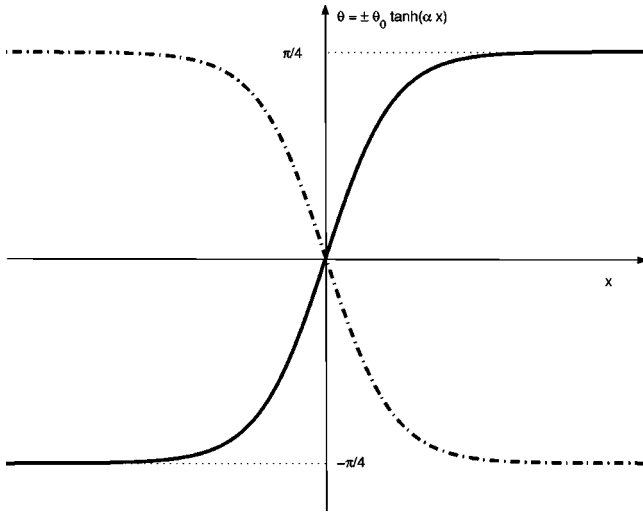


FIG. 6. Representation of a domain wall that separates the two equilibrium orientations in the sample $\theta = \pm \theta_0$. From the experimental data, we have $\theta_0 = \pi/4$.

with θ_2 being the larger of the two positive real roots of this quartic equation [19]. The Jacobi modulus k is given by $0 \leq k \equiv \theta_1 / \theta_2 \leq 1$. For the kink solution $C_0 = A^2/4B$, while for the long wavelength $\text{sn}(\cdot)$ solutions, the value of C_0 is close to it but a little less. The solutions in Eq. (22) are a set of periodic functions shown below whose period is

$$\lambda = \frac{4K(k)}{\sqrt{B/2D}} \theta_2 \tag{23}$$

and it varies depending on the ratio of θ_1 / θ_2 that defines the Jacobi modulus k . The function $K(k)$ is the so-called complete elliptic integral of the first kind [20].

In the patterns seen in Tabony's experiments, the above solutions can be identified such that we have $\lambda = 0.5$ mm which can always be satisfied by λ of Eq. (23), since $K(k) \rightarrow \infty$ as $k \rightarrow 1$. In order to get agreement with experimental observations of the striped patterns exhibiting 45° and 135° with respect to the horizontal axis, the choice of the classical turning points in Eq. (20) is dictated by $|\theta_2| \approx |\theta_1| \approx \pi/4$ (Fig. 8). Hence, $k = 1 - \epsilon$ where $\epsilon = (\theta_2 - \theta_1) / \theta_2$. Note that as $k \rightarrow 1$,

$$K(k) \approx \ln\left(\frac{4}{1-k^2}\right) + \frac{1}{4} \left[\ln\left(\frac{4}{1-k^2}\right) - 1 \right] (1-k^2) \approx -\ln \epsilon.$$

Hence,

$$\lambda \approx -\pi \ln \epsilon \sqrt{\frac{2D}{B}} \approx 0.5 \text{ mm}. \tag{24}$$

The parameters used in the above model can be independently estimated using some general properties of the obtained solutions when we compare them with the experimental observations considered here [2,6]. First of all, if D is taken to represent the rotational diffusion coefficient D_R in

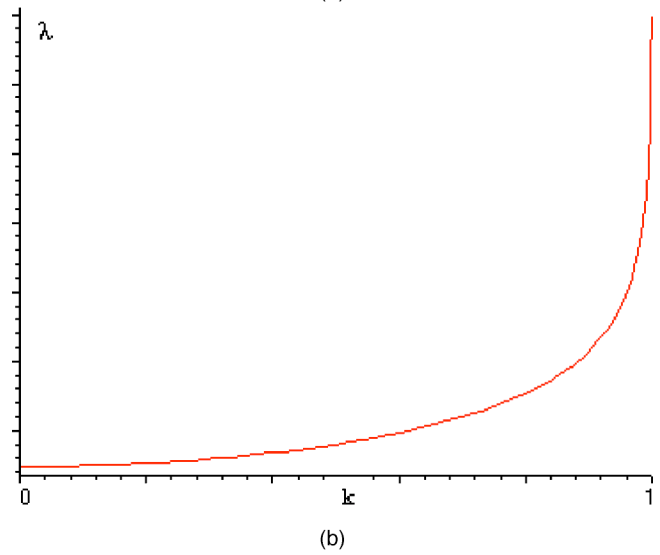
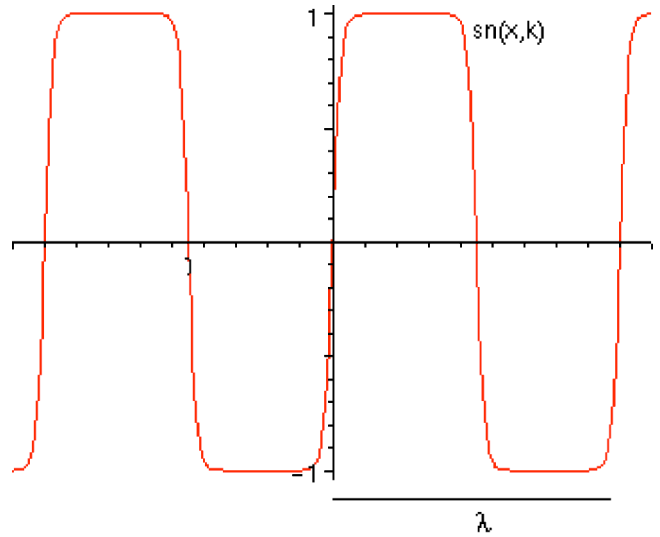


FIG. 7. (a) $\text{sn}(x,k)$ where $k=0.9998$. (b) λ as a function of k , Eq. (24).

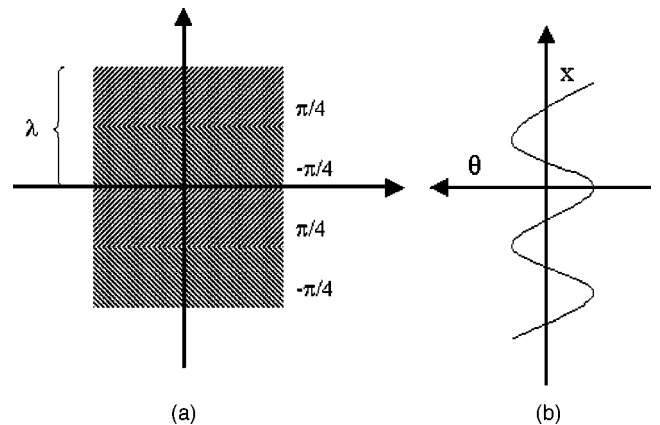


FIG. 8. (a) An illustration of orientational striped patterns with wavelength λ . (b) The director angle θ as a function of position along the vertical axis.

the presence of the other polymers, it may be obtained from the Stokes-Einstein formula as

$$D_R = \frac{k_B T}{\psi_R}, \quad (25)$$

where ψ_R is the rotational drag coefficient given by

$$\psi_R = \frac{\frac{1}{3} \pi \eta L^3}{\ln(L/r) - 0.66} \quad (26)$$

for a cylindrical MT of length L and diameter r [21]. The viscosity coefficient η of the buffer is similar to that of water, so we take $\eta = 10^{-3}$ N s/m². In our case $L = 5$ μ m and $r = 25$ nm, so that the value for D_R is $D_R^0 = 0.16$ rad²/s. However, due to the very high density of MT's in the sample, the above value is valid only for an isolated MT at dilute concentrations. In order to estimate the experimentally observed rotational diffusion coefficient, we correct the value of D_R^0 by a crowding correction [22] to give

$$D_R \approx D_R^0 (\nu L^3)^{-2}, \quad (27)$$

where ν is the density of MT's which will be taken to be $\nu = 3 \times 10^{18}$ m⁻³ [2]. This gives $D_R = 10^{-6}$ rad²/s.

By assuming k very close to unity, i.e., $k = 0.9998$, we obtain $-\ln(\epsilon) \approx 10$. Thus from Eq. (24) we can estimate B as $B \approx 6600$ rad² s⁻¹ m⁻². From the expression for θ_0 we can then determine $A \approx 4000$ rad² s⁻¹ m⁻². From this we can estimate α in the kink solution of Eq. (21) as $\alpha = 4.4 \times 10^4$ m⁻¹, thus giving the width of the transition area (domain wall) between the two adjacent acute and obtuse stripes as $1/\alpha \approx 22$ μ m. Finally from the expression for β , as $|\theta_2| \approx \pi/4$, we estimate β to be $\beta \approx 4.5 \times 10^4$ m⁻¹.

Hence, this model is sufficiently general to reproduce the experimental data. However, this model is not intended only to describe the experiments already performed. It can also be used to make predictions regarding future experiments. In particular, we can make the following predictions. Since lowering the ionic concentration reduces electrostatic screening and lowers the rotational diffusion coefficient due to the MT repulsion, we expect λ to be lowered as a result of decreasing the salt content. Conversely, increasing the salt content should lead to patterns of MT's with a shorter wavelength. The same outcome should also hold for pH changes.

Varying the temperature should have a small and opposite effect to those described above. We encourage experimentalists to try and carry out experiments whose results can either support or refute our predictions.

IV. DISCUSSION

The motivation for the present study was to describe theoretically a series of effects on MT self-organization due to the gravitation field. Tabony and co-workers [2,6] showed experimentally that the *in vitro* self-organization of MT's is crucially dependent on the gravitational field strength and the orientation of samples with respect to the gravity axis. Under gravity, striped patterns of MT's oriented consecutively at acute and obtuse angles appeared, whereas in weightlessness no pattern formation arises and MT's self-organize into an isotropic configuration without preferential orientation. The present paper provides theoretical support for these observations through the development of a model based on the relevant chemical kinetics of tubulin assembly, diffusion processes of MT's and tubulin, and the gravitational drift of MT's. In this first regime, the nucleation kinetics resulted in the formation of avalanche correlated clusters and our model predicts the emergence of a domino effect where a solitary wave of assembly propagates through the sample. We also show that the appearance of the dissipative structure correlates to the size of the sample. The second regime concerns the state of fully assembled MT's whose slow rotational diffusion is modeled through the use of a Landau-Ginzburg free energy functional. We demonstrate that free energy minimization leads to orientational ordering in the form of striped patterns that were experimentally observed and whose physical properties can be readily fitted to our model with realistic independently verified parameters. Further experiments are required to confirm our predictions and further refine the model. Finally, we made predictions regarding the behavior of this model with respect to salt concentration, pH and temperature changes.

ACKNOWLEDGMENTS

This project has been supported by grants from NSERC and MITACS. S.P. acknowledges support from the Bhatia Fund. J.M.D. would like to thank the staff and members of the Physics Department of the University of Alberta, for all their kindness and thoughtfulness during his stay.

[1] A. Desai and T.J. Mitchison, *Annu. Rev. Cell Dev. Biol.* **13**, 83 (1997).
 [2] C. Papaseit, N. Pochon, and J. Tabony, *Proc. Natl. Acad. Sci. U.S.A.* **97**, 8364 (2000).
 [3] J. Tabony and D. Job, *Proc. Natl. Acad. Sci. U.S.A.* **89**, 6948 (1992).
 [4] M.L. Lewis, J.L. Reynolds, L.A. Cubano, J.P. Hatton, B.D. Lawless, and E.H. Piepmeier, *FASEB J.* **12**, 1007 (1998).
 [5] J. Vassy, S. Portet, M. Beil, G. Millot, F. Fauvel-Lafeve, A. Karniguian, G. Gasset, T. Irinopoulou, F. Calvo, J.P. Rigaut, and D. Schoevaert, *FASEB J.* **15**, 1104 (2001).

[6] J. Tabony, *Science* **264**, 245 (1994).
 [7] T. Hill, *Linear Aggregation Theory in Cell Biology* (Springer-Verlag, Berlin, 1987).
 [8] F. Oosawa and S. Asakura, *Thermodynamics of the Polymerization of Protein* (Academic Press, New York, 1975).
 [9] D.K. Kondepudi, *Physica A* **115**, 552 (1982).
 [10] H. Flyvbjerg, E. Jobs, and S. Leibler, *Proc. Natl. Acad. Sci. U.S.A.* **93**, 5975 (1996).
 [11] E. Jobs, D.E. Wolf, and H. Flyvbjerg, *Phys. Rev. Lett.* **79**, 519 (1997).
 [12] A.E. Gonzalez, *J. Phys.: Condens. Matter* **14**, 2335 (2002).

- [13] E. Salmon, W. Saxton, R. Leslie, M. Karow, and J. McIntosh, *J. Cell Biol.* **99**, 2157 (1984).
- [14] J. Tuszynski, M.V. Sataric, S. Portet, and J.M. Dixon (unpublished).
- [15] J.A. Tuszynski, M. Otwinowski, and J.M. Dixon, *Phys. Rev. B* **44**, 9201 (1991).
- [16] D. Sept, H.J. Limbach, H. Bolterauer, and J.A. Tuszynski, *J. Theor. Biol.* **197**, 77 (1999).
- [17] P.W. Anderson, *Basic Notions of Condensed Matter Physics* (Benjamin/Cummings, Menlo Park, CA, 1984).
- [18] P. Winternitz, A.M. Grundland, and J.A. Tuszynski, *J. Phys. C* **21**, 4931 (1988).
- [19] P. F. Byrd and M. D. Friedman, *Handbook of Elliptic Integrals for Engineers and Scientists* (Springer, Berlin, 1971).
- [20] M. Abramowitz and I.A. Stegun, *Handbook of Mathematical Functions*, Natl. Bur. Stand. Appl. Math. Ser. Vol. 55 (U.S. GPO, Washington, D.C., 1964).
- [21] J. Howard, *Mechanics of Motor Proteins and the Cytoskeleton* (Sinauer Associated Inc., Sunderland, MA, 2001).
- [22] M. Doi and S. Edwards, *The Theory of Polymer Dynamics* (Oxford University Press, Oxford, 1986).